Ultra-High-Speed 2:1 Digital Selector and Plasmonic Modulator IM/DD Transmitter Operating at 222 GBaud for Intra-Datacenter Applications

Wolfgang Heni, Benedikt Baeuerle, Haïk Mardoyan, *Senior Member, IEEE*, Filipe Jorge, Jose Manuel Estaran, *Member, IEEE*, Agnieszka Konczykowska, *Fellow, IEEE*, Muriel Riet, Bernadette Duval, Virginie Nodjiadjim, Michel Goix, Jean-Yves Dupuy, *Senior Member, IEEE*, Marcel Destraz, Claudia Hoessbacher, Yuriy Fedoryshyn, Huajun Xu, Delwin L. Elder, Larry R. Dalton, *Senior Member, IEEE*, Jeremie Renaudier, *Member, IEEE*, and Juerg Leuthold, *Fellow, IEEE*

(Post-Deadline Paper)

***Abstract*—We demonstrate a 222 GBd on-off-keying transmitter in a short-reach intra-datacenter scenario with direct detection after 120 m of standard single mode fiber. The system operates at net-data rates of >200 Gb/s OOK for transmission distances of a few meters, and >177 Gb/s over 120 m, limited by chromatic dispersion in the standard single mode fiber. The high symbol rate transmitter is enabled by a high-bandwidth plasmonic-organic hybrid Mach–Zehnder modulator on the silicon photonic platform that is ribbon-bonded to an InP DHBT 2:1 digital multiplexing selector. Requiring no driving RF amplifiers, the selector directly drives the modulator with a differential output voltage of 622 mV_{pp} measured across a 50 Ω resistor. The transmitter assembly occupies a footprint of less than 1.5 mm × 2.1 mm.**

***Index Terms*—Data center, direct detection, heterogeneous integration, indium phosphide, integrated optics, intensity modulation, optical transmitter, optoelectronics, plasmonics, silicon photonics.**

Manuscript received December 6, 2019; revised January 31, 2020; accepted February 3, 2020. Date of publication February 12, 2020; date of current version May 6, 2020. This work was supported in part by the European Commission through the H2020 project QAMeleon under Grant 780354 and the H2020 project plaCMOS under Grant 98099, and in part by the Air Force Office of Scientific Research under Grant FA9550-19-1-0069. *(Benedikt Baeuerle and Wolfgang Heni contributed equally to this work). (Corresponding author: Wolfgang Heni.)*

Wolfgang Heni, Benedikt Baeuerle, Marcel Destraz, and Claudia Hoessbacher are with Polariton Technologies Ltd., 8038 Zurich, Switzerland, and also with the ETH Zurich, 8092 Zurich, Switzerland (e-mail: wolfgang@polariton.ch; benedikt@polariton.ch; destrazm@student.ethz.ch; claudia@polariton.ch).

Haïk Mardoyan, Jose Manuel Estaran, and Jeremie Renaudier are with Nokia Bell Labs, 91620 Nozay, Fance (e-mail: haik.mardoyan@nokia-bell-labs.com; jose_manuel.estaran_tolosa@nokia-bell-labs.com; jeremie.renaudier@nokia-bell-labs.com).

Filipe Jorge, Agnieszka Konczykowska, Muriel Riet, Bernadette Duval, Virginie Nodjiadjim, Michel Goix, and Jean-Yves Dupuy are with III-V Lab, 91676 Palaiseau, France (e-mail: filipe.jorge@3-5lab.fr; agnieszka.konczykowska@3-5lab.fr; muriel.riet@3-5lab.fr; bernadette.duval@3-5lab.fr; virginie.nodjiadjim@3-5lab.fr; michel.goix@3-5lab.fr; jean-yves.dupuy@3-5lab.fr).

Yuriy Fedoryshyn and Juerg Leuthold are with ETH Zurich, 8092 Zurich, Switzerland. (e-mail: yuriy.fedoryshyn@ief.ee.ethz.ch; juerg.leuthold@ief.ee.ethz.ch).

Huajun Xu, Delwin L. Elder, and Larry R. Dalton are with the University of Washington, Seattle, WA 98195-1700, USA (e-mail: hjx@uw.edu; elderdl@uw.edu; dalton@chem.washington.edu).

Color versions of one or more of the figures in this article are available online at https://ieeexplore.ieee.org.

Digital Object Identifier 10.1109/JLT.2020.2972637

I. Introduction

DRIVEN by unprecedented demand for video streaming, cloud-based services, and supercomputing as well as by the prospect of augmented reality applications, telemedicine and the Internet of Things, new optical interconnects are developed with great effort [1]. In particular, cost-, power-, and space-efficient short-reach links enabling capacities beyond 100 Gb/s are most-relevant for future intra-datacenter and rack-to-rack optical links, covering distances from a few meters up to a few kilometers.

In order to enable these short-reach links in a simple and cost-effective way, intensity modulated (IM) and direction detection (DD) systems are typically preferred.

Power-efficient, high-bandwidth, and compact electro-optic (EO) modulators are indispensable for the next generation of optical transceivers applied in these short-reach links. To ensure cost-efficiency, the number of parallel lanes should be kept small and their modulation format as simple as possible. Therefore, future optical transceivers need to deploy EO modulators with bandwidths that are significantly beyond 100 GHz to avoid any inverse multiplexing at the EO interface [1]. Besides, such modulators should be realized with a micrometer-scale footprint to still ensure a high degree of parallelization to increase the aggregate data rate of the module and to match with the dimensions of electronic driving circuitry [2]. To realize densely integrated transceivers a low power load is required [3], [4], which can be realized by modulators with low driving voltages and the avoidance of electrical 50 Ω terminated transmission lines [5], [6].

A broad variety of EO modulator technologies with ultra-large EO bandwidths has already been demonstrated. Modulators can be partitioned as electro-absorption modulators (EAMs), ring

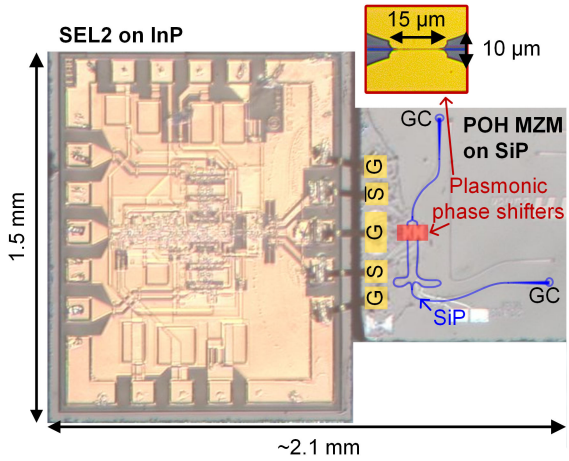

Fig. 1. 222 GBd transmitter assembly consisting of an InP DHBT 2:1-digital selector (SEL) and plasmonic organic-hybrid (POH) Mach–Zehnder modulator (MZM) on silicon photonics. The RF electrodes of the modulator are ribbon-bonded to the output stage of the SEL. The assembly requires less than $2.1 \times 1.5\text{-mm}^2$.

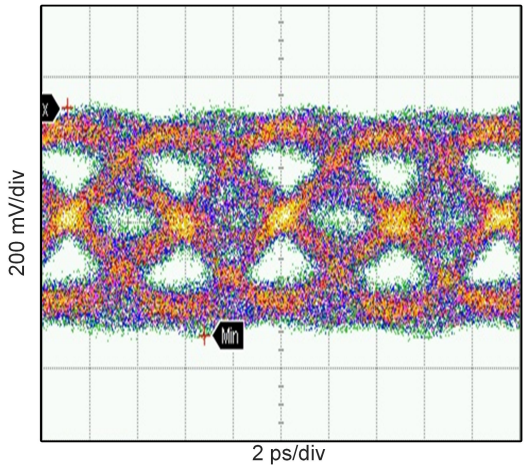

Fig. 2. 2:1 multiplexing selector electrical output at 222 GBd OOK with a peak-to-peak voltage of 622 mV_{pp}, measured with probe tips at in- and output.

resonator modulators (RRMs), and Mach-Zehnder modulators (MZMs). The EAM concept has been proved mainly on two platforms, indium phosphide [3], [4] and germanium silicon [7], [8]. The RRM implementation has been realized on the silicon photonics platform [9] with a bit-rate beyond 100 Gbit/s and on the plasmonic-organic hybrid platform [10] with an EO bandwidth beyond 100 GHz. The MZM concept has been demonstrated on different technology platforms including lithium niobate [11], [12], silicon photonics [13], [14], silicon-organic hybrid [15], indium phosphide [16], [17], polymer photonics [18], [19], and plasmonics [20], [21].

While there are many promising modulator technologies available, only few support highest symbol rates, and up to now, only complex IM/DD transmitters beyond 200 Gb/s have been demonstrated. Constrained by bandwidth-limited components, the modulation of multiple bits per symbol [4], [12], [14], [21], [22], the discrete multi-tone (DMT) modulation [16], [23] or the Kramers-Kronig (KK) technique [24], [25] can help to achieve bit-rates beyond 200 Gb/s per wavelength. However, this comes at the price of advanced DSP or additional electrical and optical components.

In this work, we demonstrate a low-complexity 222 Gb/s OOK per wavelength transmitter and test its performance in a short-reach (up to 120 m) direct-detection link. This work is an extension of the post-deadline paper presented at ECOC 2019 in Dublin [26]. Enabled by the combination of a >100 GHz-bandwidth plasmonic-organic hybrid (POH) Mach-Zehnder modulator on silicon photonics and an InP DHBT 2:1 selector, the transmitter generates an OOK signal at a record symbol rate of 222 GBd over 120 m standard single mode fiber in an intra-data center infrastructure scenario.

II. 222 GBd Transmitter

The 222 GBd transmitter is depicted in Fig. 1. It consists of a high-speed 2:1 multiplexing selector (SEL) and a POH MZM, fabricated on silicon photonics. To overcome packaging-related bandwidth limitations, the POH MZM was bonded to the SEL using 25-µm-wide gold ribbon bonds in a GSGSG configuration that had lengths below 200 µm. This way, the transmitter enables to benefit from the high performance of the individual components with minor performance penalties imposed by the electrical interfacing.

In addition to the high symbol rate performance, the transmitter offers a compact footprint of below 3.15 mm², dominated by the electrical chip and bonding electrodes. The POH MZM occupies a footprint of less than 0.05 mm², the active plasmonic area itself less than 0.006 mm^2.

A. High-Speed 2:1 Multiplexing Selector

The high-speed 2:1 multiplexing selector [27], [28] was fabricated in III-V Lab's 0.7 µm indium phosphide (InP) double-heterojunction bipolar transistor (DHBT) technology, optimized for a broad data-bandwidth up to symbol rates beyond 200 GBd. The transistors used to design and fabricate the selector have characteristic gain-bandwidth-product-related frequencies f_{T} and f_{max} around 400 GHz, with a DC current gain around 30 [27], [28].

In a first characterization at 212 Gb/s, with state-of-the-art 122 GHz remote sampling heads from Keysight (N1046A-12F), the SEL chip already demonstrates its performance with a signal-to-noise ratio of ~7 and a jitter of $T_{\text{jitter,rms}} = 300$ fs at an output voltage of 240 mV_{pp} [27]. The differential output amplitude at 212 GBd can be adjusted between 240 $\text{mV}_{\text{ppdiff}}$ and 730 $\text{mV}_{\text{ppdiff}}$, resulting in a circuit power consumption of 0.5 W and 0.8 W, respectively. Fig. 2 shows the measured electrical output signal of the 2:1 multiplexing selector at a symbol rate of 222 GBd, here measured with regular 70-GHz-bandwidth Keysight 86118A remote sampling heads, with a measured peak-to-peak voltage of 622 $\text{mV}_{\text{ppdiff}}$, used in this work. The voltage was measured using electrical probes at both the input and the output of the module.

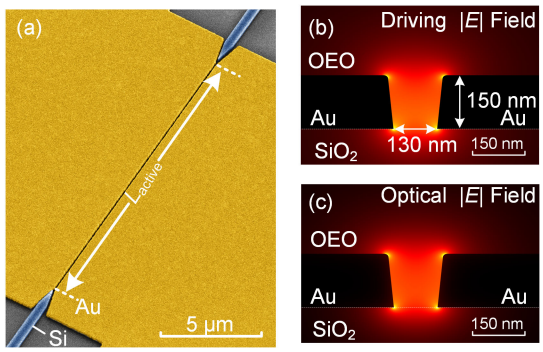

Fig. 3. (a) Colorized scanning electron microscope picture of a plasmonic phase modulator. (b-c) Simulated electric field distribution of the (b) driving single and the (c) plasmonic mode in the slot waveguide. Figures are adapted from [33].

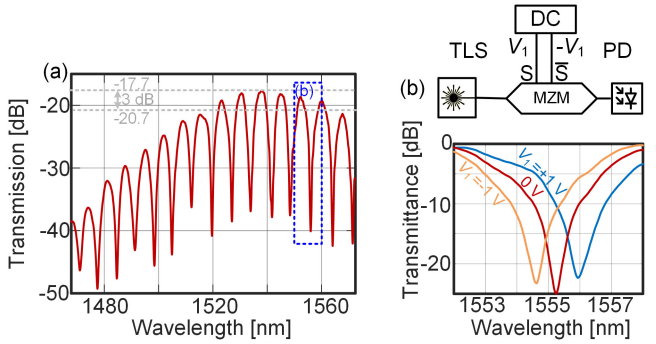

Fig. 4. (a) Modulator transmission spectrum. (b) Voltage-dependent tuning of the operating point.

B. High-Speed Plasmonic Modulator

The high-speed plasmonic modulator consists of a plasmonic-organic hybrid (POH) Mach-Zehnder modulator that is fabricated on the silicon photonic (SiP) platform. The POH MZM combines the low-loss SiP technology, the extreme light-confinement of plasmonics, and highly efficient organic electro-optic materials. This way, it offers EO modulation with EO bandwidths beyond 500 GHz [29], an optical operating range between 1200 nm and >1600 nm [30] and micrometer footprints [31]. The active section of the MZM consists of two plasmonic phase modulators (PPMs) [32] that are connected in a dual-drive configuration [20]. A colorized scanning electron microscope (SEM) picture of a PPM is depicted in Fig. 3(a) [33]. It consists of two gold electrodes separated by a narrow gap of ∼130 nm, forming the plasmonic slot waveguide. The gap is filled with an organic electro-optic (OEO) material. When an electric signal is applied to the gold electrodes, the electric field drops across the nanoscale slot (Fig. 3(b)), modulating the refractive index of the OEO material. Light is fed in via silicon photonic waveguides to the plasmonic section, where the light is guided as surface plasmon polaritons (SPPs) along the metallic waveguide. The light is tightly confined within the OEO material (Fig. 2(c)), efficiently translating the refractive index modulation into a phase modulation [34]. In this work, the PPMs are filled with the organic electro-optic material composite 2:1 HLD1:HLD2. In thin-film experiments, the material shows stable performance over >500h at 85 °C [35].

By integrating the PPMs in a SiP Mach-Zehnder interferometer configuration, the phase modulation is translated into an amplitude or intensity modulation. These MZMs [36] can be used for radio-over-fiber applications and THz communication [29], [37], 200 Gbit/s intensity modulation [21] , 120 GBd IM with sub-1V_{pp} driving electronics [20] as well as highly spatially parallelized modulator arrays for space-division multiplexing (SDM) and wavelength division multiplexing (WDM) applications [38], [39].

Furthermore, when implemented in a nested Mach-Zehnder configuration, they offer most-compact 100 GBd complex modulation [33], [40] with sub-1V_{pp} driving electronics and efficient 400 Gb/s modulation on SiP [33].

The large EO bandwidth of the POH modulator is enabled by the compact size of the modulator. The merely 15 µm long active section leads to a modulator capacitance of ∼7 fF [33]. In combination with the fact, that the gold slot-waveguide also forms the contacting electrodes, this results in extremely small RC time constants, thus, enabling the EO bandwidth >500 GHz [29].

In this work, the plasmonic MZM was implemented in a dual-drive configuration [20]. In this configuration, the plasmonic modulator makes efficient use of the provided driving signal, removing the need for power-hungry electrical driving amplifiers. The plasmonic dual-drive implementation allows increasing the effective voltage dropping across the active section by a factor of 4, compared to a traditional 50 Ω terminated modulator for two reasons. First, our plasmonic MZMs are implemented as purely capacitive, open circuit devices. When driven by a 50 Ω-matched signal source, twice the 50 Ω-measured voltage applies at the device. Second, an additional doubling of the voltage is achieved by applying the differential signal across the plasmonic slot. This way, a single-ended driving voltage of only $V_\pi/4$ is required to fully drive the modulator [20].

The plasmonic MZM has an on-chip loss of 9.7 dB, and a total fiber-to-fiber loss of 17.7 dB (4 dB per grating coupler). Note than both the on-chip losses and the fiber-to-fiber losses can be further improved to below 10 dB, when applying industrial coupling and fabrication techniques [33]. When considering standard edge-couplers with 1.5 dB/coupler [41], fiber-to-fiber losses can be reduced by ∼5 dB. Dedicated fabrication processes and optimized organic electro-optic materials can further reduce the fiber-to-fiber losses [33], [42]. The MZM is implemented in an imbalanced configuration implemented in SiP, see Fig. 1, in order to adjust the operating point by choosing the operating wavelength.

It furthermore features a SiP thermo-optic phase shifter to adjust the operating point. Fig. 4(a) shows the optical transmission spectrum of the modulator. The MZM has an extinction ratio exceeding 20 dB, the fiber-to-chip grating couplers impose a 3 dB optical bandwidth of 1520 nm to ∼1565 nm. Fig. 4(b) depicts the DC dependent modulator operating point, measured using a tunable laser source. A voltage $V_1 = \pm 1$ V $= -V_2$ is applied to the modulator's signal (S) electrode, shifting the operating point by approximately 0.4 π. This corresponds to

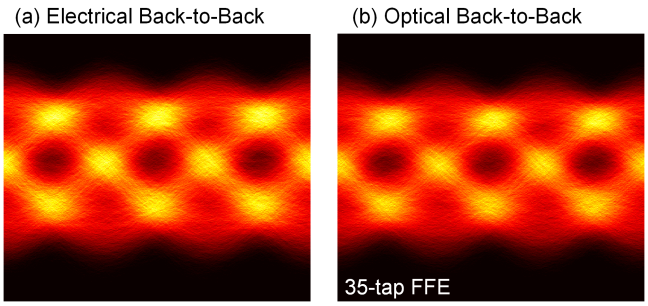

Fig. 5. 222 GBd OOK eye diagrams recorded in the DSO. (a) Electrical back-to-back before post-processing. (b) Optical back-to-back with a 35-tap FFE.

on-off-voltages of $V_1 = \pm 2.7\,\mathrm{V} = -V_2$ and $V_\pi = 10.8\,\mathrm{V}$. Note that when using 50 Ω-matched signal source a single-ended driving voltage of 2.7 V is needed to fully switch the modulator from off to on [20]. With the 622 $\mathrm{mV_{ppdiff}}$ 50 Ω-matched driving voltage provided by the 2:1 multiplexing selector, the modulator provides a ER of ∼7.5 dB when operated in the 3 dB point, see Fig. 4(b). The purely capacitive MZM consumes only the energy required to charge / discharge the device capacitance. With a capacitance of ∼7 fF [20] (∼40 fF including bonding electrodes [33]) and a driving voltage of 622 $\mathrm{mV_{ppdiff}}$, the electrical energy consumption per bit calculates to 11 fJ/bit (62 fJ/bit) [20].

III. Demonstration of 222 GBd Transmission

The 222 GBd transmitter was tested in short-reach IM/DD scenario with transmission lengths of up to 120 m of standard single mode fiber (SSMF).

A. Experimental Setup

Fig. 6 depicts the experimental setup of the modulation experiment. The 222 GBd signal is generated by three stages. First, two 55.5 Gb/s pseudo-random bit sequences (PRBS, word length 2^{11}) are generated by a pattern generator. Second, a first 2:1 selector (SEL1) generates a 111-Gb/s output signal that is, third, fed into the probed 2:1 selector (SEL2), generating the 222 GBd driving signal with a maximum output amplitude of 622 $\mathrm{mV_{ppdiff}}$. The selectors and the bit pattern generator are clocked by a clock distribution platform with (Bit Rate: BR): BR/8 for BPG, BR/4 for SEL1 and BR/2 for SEL2. The electrical clocks were synchronized by a 10 MHz reference time base.

A laser with $\lambda = 1541.9$ nm was coupled to and from the transmitter using silicon grating couplers interfaced by cleaved SSMFs. The laser wavelength was chosen in order to operate the MZM close to the 3 dB operating point. An erbium doped fiber amplifier (EDFA) amplified the optical signal before it was sent into the SSMF transmission line.

In the receiver, the optical signal was band-pass filtered (400 GHz) before it was amplified, adjusted in power using a variable optical attenuator (VOA), and detected by a 100 GHz photo diode. The optical 222 GBd spectrum before reception is displayed as an inset in Fig. 6. The received signal was then recorded by a 256 GS/s Keysight Infiniium digital storage oscilloscope (DSO) with an electrical bandwidth of 113 GHz. The recorded spectrum in the DSO is displayed as an inset in Fig. 6. The signal was then evaluated after digital signal processing (DSP), followed by bit error rate (BER) calculation. The DSP included resampling, timing recovery, and demodulation.

Fig. 5 displays the 222 GBd back-to-back eye diagram measured in the receiver for the electrical (a) and the optical (b) back-to-back. Note that the electrical back-to-back was recorded with a 1 m long RF cable connectorized with 1.85 mm coaxial connectors.

B. 222 GBd Transmission

The 222 GBd transmission performance was studied using different equalizer modes and sweeping the receiver optical power (ROP) from −1 dBm to 12 dBm. In order to understand the origin of signal distortions at 222 GBd the influence of the equalizer complexity was investigated. To find a satisfactory compromise between performance and processing complexity, feed-forward equalizer (FFE) taps were swept up to 55 taps , the lookup table (LUT) memory up to 7 symbols.

Fig. 7 plots the measured BER versus received optical power (ROP) into the photodetector. For comparison, the BER thresholds of the 10%−, 25%− and 33%-overhead hard-decision staircase forward error correction (FEC) codes in [43], with pre-FEC BER limits at 7.5×10^{-3}, 1.82×10^{-2} and 2.24×10^{-2} respectively, are added.

The transmitter enables the successful transmission of 222 GBaud serial OOK signals over more than 120 m of SSMF.

The system operates at net-data rates of >200 Gb/s OOK in the back-to-back scenario, and >177 Gb/s over 120 m, limited by chromatic dispersion (CD) in the standard single mode fiber.

CD in the SSMF is major challenge for data transmission at highest symbol rates, in case of the 222 GBd signal requiring an optical bandwidth >150 GHz. However, even with a measured CD transmission penalty of >5 dB, the proposed scheme performs below the 25%-overhead FEC limit, enabled by the high signal quality of the 222 GBd transmitter.

Limited by chromatic dispersion, the performance after 120 m transmission over SSMF saturates around the 25%-overhead HD-FEC limit. For low-complexity DSP (35-tap FFE, 3-symbol LUT) a BER below the 33%-overhead HD-FEC limit is only achieved for a high receiver optical power of 12 dBm. When increasing the LUT length to 5 symbols, the performance reaches the 25%-overhead HD-FEC limit. This may cause challenges in practical applications, e.g., when system variations may slightly increase the BER above the 25%-overhead HD-FEC limit. The performance can be improved further by 3 dB compared to the 5-symbol LUT, when considering a 7-symbol LUT. This way, the BER stays clearly below 1.82×10^{-2} and enables, with a 4 dB operation margin, an input-power tolerant operation with 25% overhead and a net-rate of 170 Gb/s. Furthermore, increasing the LUT-length reduces the CD penalty to only 3.5 dB. The overlapping BER curves of the 35-tap FFE and the 55-tap FFE show that no significant gain in performance can be achieved by increasing the complexity of the linear compensation filter. Consequently, the performance degradation in the system is

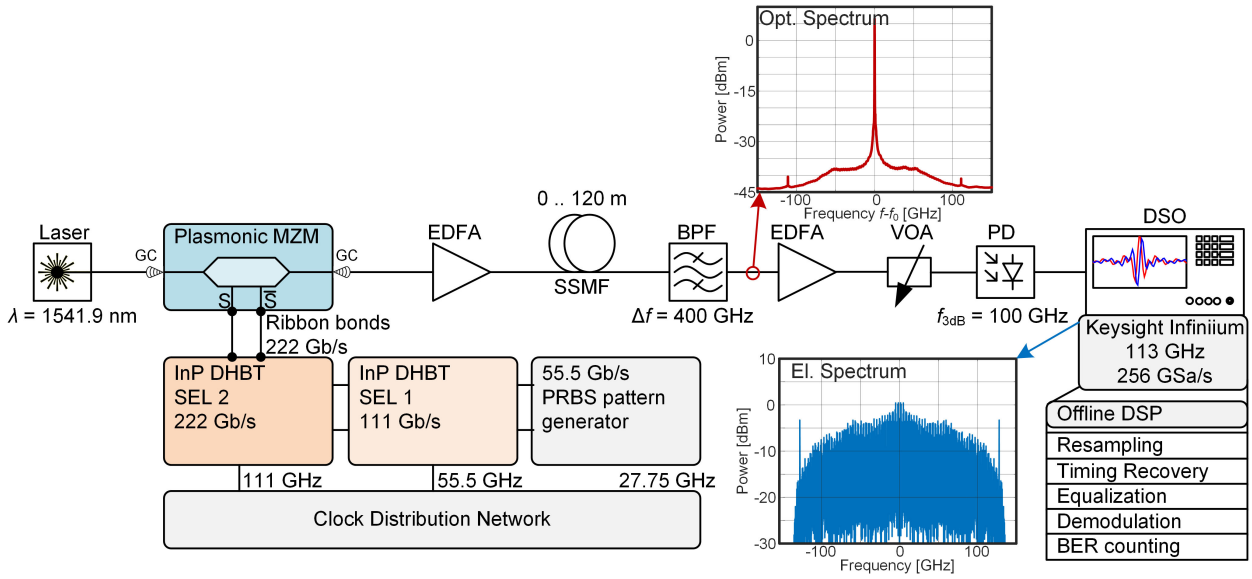

Fig. 6. Experimental setup for 222 GBd back-to-back and 120 m transmission experiment. Light is coupled to and from the plasmonic MZM using silicon photonic grating couplers (GCs). The 222 GBd electrical signal is applied to the MZM using ribbon bonds between 2:1 selector chip (SEL2) and the MZM. Insets: Optical and electrical modulation spectra. The optical modulation spectrum at 222 GBd OOK NRZ in the back-to-back scenario. The electrical modulation spectrum in the back-to-back scenario as recorded by the DSO.

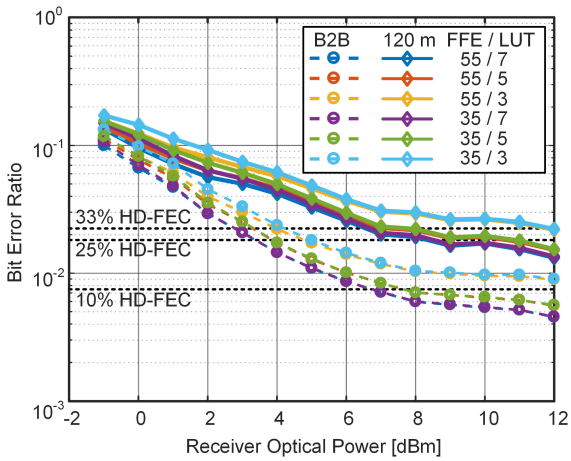

Fig. 7. 222 GBd performance for back-to-back (B2B) and for transmission over 120 m SSMF. BER as a function of the receiver optical power for different feed-forward equalizer taps and lookup table memories. Considering forward error correction, net-data rates of >177 Gb/s for 120 m transmission and >200 Gb/s in the back-to-back scenario are demonstrated.

dominated by non-linear distortion confirmed by the improved BER performance with increasing LUT sizes.

When analyzing the influence of the receiver optical power on the BER, an error floor starting at ∼8 dBm ROP is observable (see Fig. 7). For a reasonable DSP configuration of a 35-tap FFE and a 5-symbol LUT, the back-to-back scenario stays below the 10%-overhead HD-FEC limit [43]. When the least-complex DSP is used (35-tap FFE, 3-symbol LUT), the BER saturates below $<1 \times 10^{-2}$, still allowing for 25%-overhead HD-FEC.

Using Fig. 7, performance of shorter transmission distances of e.g., a few meters can be estimated. With simple DSP of 35 FFE taps and a 3-symbol LUT, which can be processed already by today's 25 to 50 GBd multilevel modules, net-rates of more than 177 Gb/s can be achieved with simple OOK and an ROP of >5 dB. Allowing for more-complex DSP of 35 FFE taps and a 5-symobl LUT, the system performs at a net-rate of more than 200 Gb/s using OOK and a direct detection receiver can be achieved.

IV. Conclusion

We demonstrate an on-off keying optical transmitter operating at a symbol rate of 222 GBd. The transmitter is tested in a short-reach scenario with a transmission distance of up to 120 m over standard single mode fiber. By relying on a standard direct-detection optical receiver, no DSP on transmitter side and standard DSP on receiver side, we demonstrate a power- and cost efficient high-speed solution for intra-datacenter applications.

For transmission distances of 120 m, we report net-data rates between 160 Gb/s and 180 Gb/s using a 5- or 7-symbol LUT, respectively. The net data rate is limited by chromatic dispersion in the standard single mode fiber. When considering transmission distances of only a few meters, net-rates of 177 Gb/s using simple DSP with a 3-symbol LUT are shown. When increasing the symbol length to 7, a net-rate of more than 200 Gb/s using on-off keying and direct detection is demonstrated.

The record-high symbol rate transmission was enabled by the side-by-side assembly of a plasmonic-organic hybrid Mach-Zehnder modulator fabricated on the silicon photonics platform, directly driven by the differential 622 mV_{pp} data stream provided by an ultra-high-speed 2:1 InP DHBT selector, without any need for driving RF amplifiers. Occupying a footprint of less than 2.1 × 1.5-mm², this transmitter not only provides the highest symbol rate to date, but may be a compact, space- and cost-efficient solution for short-reach interconnect applications such as supercomputing, for intra-data center applications, rack-to-rack communications and potentially even board-to-board communications.

ACKNOWLEDGMENT

The authors thank Keysight for the loan of equipment.

REFERENCES

[1] P. J. Winzer and D. T. Neilson, "From scaling disparities to integrated parallelism: A decathlon for a decade," *J. Lightw. Technol.*, vol. 35, no. 5, pp. 1099–1115, Mar. 2017.

[2] C. Minkenberg *et al.*, "Reimagining datacenter topologies with integrated silicon photonics," *J. Opt. Commun. Netw.*, vol. 10, no. 7, pp. B126–B139, Jul. 2018.

[3] J. M. Estaran *et al.*, "140/180/204-Gbaud OOK transceiver for inter- and intra-data center connectivity," *J. Lightw. Technol.*, vol. 37, no. 1, pp. 178–187, Jan. 2019.

[4] S. Kanazawa *et al.*, "214-Gb/s 4-PAM operation of flip-chip interconnection EADFB laser module," *J. Lightw. Technol.*, vol. 35, no. 3, pp. 418–422, Feb. 2017.

[5] D. A. B. Miller, "Attojoule optoelectronics for low-energy information processing and communications," *J. Lightw. Technol.*, vol. 35, no. 3, pp. 346–396, Feb. 2017.

[6] R. Urata, H. Liu, L. Verslegers, and C. Johnson, "Silicon photon. technologies: Gaps analysis for datacenter interconnects," in *Silicon Photonics III*, Berlin, Germany: Springer, 2016, pp. 473–488.

[7] J. Verbist *et al.*, "Real-Time 100 Gb/s NRZ and EDB transmission with a GeSi electro-absorption modulator for short-reach optical interconnects EAM," *J. Lightw. Technol.*, vol. 36, no. 1, pp. 90–96, Jan. 2018.

[8] A. Melikyan, N. Kaneda, K. Kim, Y. Baeyens, and P. Dong, "100 GBaud QAM signaling with silicon photonic electro-absorption modulators," presented at the Eur. Conf. Opt. Commun. (ECOC), Dublin, Ireland, Sep. 2019.

[9] J. Sun, R. Kumar, M. Sakib, J. Driscoll, H. Jayatilleka, and H. Rong, "A 128 Gb/s PAM4 silicon microring modulator with integrated thermo-optic resonance tuning," *J. Lightw. Technol.*, vol. 37, no. 1, pp. 110–115, Jan. 2019.

[10] C. Haffner *et al.*, "Low-loss plasmon-assisted electro-optic modulator," *Nature*, vol. 556, no. 7702, pp. 483–486, Apr. 2018.

[11] C. Wang *et al.*, "Integrated lithium niobate electro-optic modulators operating at CMOS-compatible voltages," *Nature*, vol. 562, no. 7725, pp. 101–104, Sep. 2018.

[12] Y. Zhang *et al.*, "220 Gbit/s optical PAM4 modulation based on lithium niobate on insulator modulator," presented at the Eur. Conf. Opt. Commun. (ECOC), Dublin, Ireland, Sep. 2019.

[13] S. Zhalehpour *et al.*, "All-silicon IQ modulator for 100 GBaud 32QAM transmissions," in *Proc. Opt. Fiber Commun. Conf. Postdeadline Papers*, San Diego, CA, USA: Optical Society of America, 2019, pp. 1–3.

[14] M. Jacques *et al.*, "200 Gbit/s net rate transmission over 2 km with a silicon photonics segmented MZM," presented at the Eur. Conf. Opt. Commun. (ECOC), Dublin, Ireland, Sep. 2019.

[15] S. Wolf *et al.*, "Silicon-organic hybrid (SOH) Mach–Zehnder modulators for 100 Gbit/s on-off keying," *Sci. Rep.*, vol. 8, no. 1, Apr 2018, Art. no. 2598.

[16] H. Yamazaki *et al.*, "IMDD transmission at net data rate of 333 Gb/s using over-100-GHz-bandwidth analog multiplexer and Mach–Zehnder modulator," *J. Lightw. Technol.*, vol. 37, no. 8, pp. 1772–1778, Apr. 2019.

[17] S. Lange *et al.*, "100 GBd intensity modulation and direct detection with an InP-based monolithic DFB laser Mach–Zehnder modulator," *J. Lightw. Technol.*, vol. 36, no. 1, pp. 97–102, Jan., 2018.

[18] V. Katopodis *et al.*, "Serial 100 Gb/s connectivity based on polymer photonics and InP-DHBT electronics," *Opt. Express*, vol. 20, no. 27, pp. 28538–28543, Dec. 2012.

[19] S. Yokoyama, G.-W. Lu, X. Cheng, F. Qiu, and A. M. Spring, "110 Gbit/s On-Off keying transmitter based on a single-drive polymer modulator," in *Proc. Opt. Fiber Commun. Conf.*, San Diego, CA, USA, 2019, pp. 1–3.

[20] B. Baeuerle *et al.*, "120 GBd plasmonic Mach–Zehnder modulator with a novel differential electrode design operated at a peak-to-peak drive voltage of 178 mV," *Opt. Express*, vol. 27, no. 12, pp. 16823–16832, Jun. 2019.

[21] B. Baeuerle *et al.*, "Reduced equalization needs of 100 GHz bandwidth plasmonic modulators," *J. Lightw. Technol.*, vol. 37, no. 9, pp. 2050–2057, May 2019.

[22] H. Mardoyan *et al.*, "84-, 100-, and 107-GBd PAM-4 intensity-modulation direct-detection transceiver for datacenter interconnects," *J. Lightw. Technol.*, vol. 35, no. 6, pp. 1253–1259, Mar. 2017.

[23] X. Chen, S. Chandrasekhar, J. Cho, and P. Winzer, "Single-wavelength and single-photodiode entropy-loaded 554-Gb/s transmission over 22-km SMF," in *Proc. Opt. Fiber Commun. Conf. Exhib.*, San Diego, CA, USA, 2019, pp. 1–3.

[24] X. Chen *et al.*, "218-Gb/s single-wavelength, single-polarization, single-photodiode transmission over 125-km of standard singlemode fiber using Kramers-Kronig detection," in *Proc. Opt. Fiber Commun. Conf. Exhib.*, 2017, pp. 1–3.

[25] S. T. Le *et al.*, "8×256 Gbps virtual-carrier assisted WDM direct-detection transmission over a single span of 200 km," in *Proc. Eur. Conf. Opt. Commun.*, Gothenburg, Sweden, 2017, pp. 1–3.

[26] H. Mardoyan *et al.*, "222-GBaud On-Off keying transmitter using ultra-high-speed 2:1 selector and plasmonic modulator on silicon photonics," presented at the Eur. Conf. Opt. Commun. (ECOC), Dublin, Ireland, Sep. 2019.

[27] A. Konczykowska *et al.*, "212-Gbit/s 2:1 multiplexing selector realised in InP DHBT," *Electron. Lett.*, vol. 55, no. 5, pp. 242–244, Mar. 2019.

[28] V. Nodjiadjim *et al.*, "0.7- um InP DHBT technology with 400-GHz f_t and f_MAX and 4.5-V BVCE0 for high speed and high frequency integrated circuits," *IEEE J. Electron. Devices Soc.*, vol. 7, pp. 748–752, Jul. 2019.

[29] M. Burla *et al.*, "500 GHz plasmonic Mach–Zehnder modulator enabling sub-THz microwave photonics," *APL Photon.*, vol. 4, no. 5, 2019, Art no. 056106.

[30] C. Haffner *et al.*, "Harnessing nonlinearities near material absorption resonances for reducing losses in plasmonic modulators," *Opt. Mater. Express*, vol. 7, no. 7, pp. 2168–2181, 2017.

[31] C. Haffner *et al.*, "Plasmonic organic hybrid modulators—Scaling highest speed photonics to the microscale," *Proc. IEEE*, vol. 104, no. 12, pp. 2362–2379, Dec. 2016.

[32] A. Melikyan *et al.*, "High-speed plasmonic phase modulators," (in English), *Nature Photon.*, vol. 8, no. 3, pp. 229–233, Mar. 2014.

[33] W. Heni *et al.*, "Plasmonic IQ modulators with attojoule per bit electrical energy consumption," *Nature Commun.*, vol. 10, no. 1, 2019, Art. no. 1694.

[34] W. Heni *et al.*, "Silicon-Organic and Plasmonic-Organic hybrid photonics," *ACS Photon.*, vol. 4, no. 7, pp. 1576–1590, 2017.

[35] H. Xu *et al.*, "Ultrahigh electro-optic coefficients, high index of refraction, and long-term stability from diels-alder crosslinkable binary molecular glasses," *Chem. Mater.*, to be published, doi: 10.1021/acs.chemmater.9b03725.

[36] W. Heni *et al.*, "108 Gbit/s plasmonic Mach–Zehnder modulator with 70-GHz electrical bandwidth," (in English), *J. Lightw. Technol.*, vol. 34, no. 2, pp. 393–400, Jan. 2016.

[37] S. Ummethala *et al.*, "THz-to-optical conversion in wireless communications using an ultra-broadband plasmonic modulator," *Nature Photon.*, vol. 13, no. 8, pp. 519–524, 2019.

[38] W. Heni *et al.*, "High speed plasmonic modulator array enabling dense optical interconnect solutions," *Opt Express*, vol. 23, no. 23, pp. 29746–29757, Nov., 2015.

[39] U. Koch *et al.*, "Ultra-compact terabit plasmonic modulator array," *J. Lightw. Technol.*, vol. 37, no. 5, pp. 1484–1491, Mar. 2019.

[40] M. Ayata *et al.*, "All-plasmonic IQ modulator with a 36 μm fiber-to-fiber pitch," *J. Lightw. Technol.*, vol. 37, no. 5, pp. 1492–1497, Mar. 2019.

[41] L. Carroll *et al.*, "Photonic packaging: transforming silicon photonic integrated circuits into photonic devices," *Appl. Sci.*, vol. 6, no. 12, 2016, pp. 1–21.

[42] B. H. Robinson *et al.*, "Optimization of plasmonic-organic hybrid electro-optics," (in English), *J. Lightw. Technol.*, vol. 36, no. 21, pp. 5036–5047, Nov., 2018.

[43] L. M. Zhang and F. R. Kschischang, "Staircase codes with 6% to 33% overhead," *J. Lightw. Technol.*, vol. 32, no. 10, pp. 1999–2002, May, 2014.